Liquid structure of shock-compressed hydrocarbons at megabar pressures

Hartley, N. J.; Vorberger, J.; Döppner, T.; Cowan, T.; Falcone, R. W.; Fletcher, L. B.; Frydrych, S.; Galtier, E.; Gamboa, E. J.; Gericke, D. O.; Glenzer, S. H.; Granados, E.; Macdonald, M. J.; Mackinnon, A. J.; Mcbride, E. E.; Nam, I.; Neumayer, P.; Pak, A.; Rohatsch, K.; Saunders, A. M.; Schuster, A. K.; Sun, P.; van Driel, T.; Kraus, D.;

Originally published:

December 2018

Physical Review Letters 121(2018)24, 245501

DOI: https://doi.org/10.1103/PhysRevLett.121.245501

Liquid Structure of Shock-Compressed Hydrocarbons at Megabar Pressures

N. J. Hartley,[1,2,*] J. Vorberger,[1] T. Döppner,[3] T.Cowan,[1,4] R. W. Falcone,[5] L. B. Fletcher,[6] S. Frydrych,[7,3] E. Galtier,[6] E. J. Gamboa,[6] D. O. Gericke,[8] S. H. Glenzer,[6] E. Granados,[6] M. J. MacDonald,[6,9] A. J. MacKinnon,[6] E. E. McBride,[6,10] I. Nam,[6] P. Neumayer,[11] A. Pak,[3] K. Rohatsch,[1] A. M. Saunders,[5] A. K. Schuster,[1] P. Sun,[6] T. van Driel,[6] and D. Kraus[1,4]

[1] *Helmholtz-Zentrum Dresden-Rossendorf, Bautzner Landstraße 400, Dresden 01328, Germany*
[2] *Open and Transdisciplinary Research Institute, Osaka University, Suita, Osaka 565-0087, Japan*
[3] *Lawrence Livermore National Laboratory, Livermore CA 94550, USA*
[4] *Technische Universität Dresden, Dresden 01062, Germany*
[5] *Department of Physics, University of California, Berkeley CA 94720, USA*
[6] *SLAC National Accelerator Laboratory, Menlo Park CA 94309, USA*
[7] *Technische Universität Darmstadt, Schlossgartenstraße 9, 64289 Darmstadt, Germany*
[8] *Centre for Fusion, Space and Astrophysics, Department of Physics, University of Warwick, Coventry CV4 7AL, United Kingdom*
[9] *University of Michigan, Ann Arbor, MI 48109, USA*
[10] *European XFEL GmbH, Holzkoppel 4, 22869 Schenefeld, Germany*
[11] *GSI Helmholtzzentrum für Schwerionenforschung GmbH, Planckstraße 1, 64291 Darmstadt, Germany*

(Dated: May 4, 2018)

We present ion structure results from hydrocarbons (polystyrene, polyethylene) shock compressed to pressures of up to 190 GPa, inducing rapid melting of the samples. The structure of the resulting liquid is then probed using *in situ* diffraction by an X-ray free electron laser beam, with precise, reliable diffraction data obtained from single shots. This is the first example of single shot diffraction from low-Z samples dynamically driven into the liquid state. The data agrees well with the structure factors calculated from *ab initio* simulations, demonstrating their ability to model mixed samples in this state. While the results exclude the possibility of complete carbon-hydrogen demixing at the conditions probed, they also, in contrast to previous predictions, demonstrate that diffraction is not always a sufficient diagnostic for this phenomenon.

Compounds and mixtures containing low-Z atoms at high pressures and temperatures are relevant to a variety of scientific fields, including planetary interiors [1–3], geophysics [4, 5] and inertial confinement fusion research [6, 7]. These often include hydrocarbons which, being formed from some of the most common elements in the universe, are commonly found as a major constituent of 'icy giant' planets [8]. In the form of plastics, hydrocarbons are also used as ablator materials in high energy density (HED) research [9], and to drive the compression in inertial confinement fusion implosions [10].

Describing compounds at high pressures and temperatures is generally complex, because the thermal energy is comparable to the binding energy, such that chemicals bond lifetimes are reduced, and longe range order is lost. It may then be energetically favourable for the mixture of various atom types to demix into separate phases with different atomic ratios [11], as with hydrogen and helium in giant planet interiors [12, 13], or the formation of diamonds within icy giants [14]. Such demixing strongly influences the energy transport in the mantle of planets with consequences for the evolution and cooling rate. If similar processes occur in inertial confinement fusion drivers, the resulting higher density liquid, or solid material, could be the source of hydrodynamic istabilities and ablator-fuel mixing at the interface [15].

While matter inside planets is gravitationally contained [16], to recreate such conditions here on Earth, other approaches must be employed. Although static compression techniques are able to cover an increasingly large region of pressure-temperature space [17, 18], the highest pressures can only be reached through dynamic compression techniques. These can include magnetically driven flier plates [19] or, as in the work presented here, laser driven shock compression [20]. While these can create high pressure and temperature states, they do so only briefly, and so the sample must be studied within the confinement time, which is on the order of ns for laser-driven shock compression.

One of the most successful approaches to studying such states uses fs-scale X-ray pulses from X-ray Free Electron Lasers (XFELs) to probe the structure of the ions within a sample by diffraction [21]. Due to the transient nature of the conditions reached in dynamic experiments, it is essential that this data can be reliably obtained from a single shot. This becomes even more important for laser-driven experiments, where significant shot-to-shot variation in the laser energy or pulse shape may ovvur. Although obtaining single-shot data is well-established for mid- to high-Z materials, which give strong diffraction signals [22, 23], and crystalline structures, which contain clear Bragg peaks [24], results from low-Z materials in the liquid state have until now only been possible by accumulating data over many shots [25].

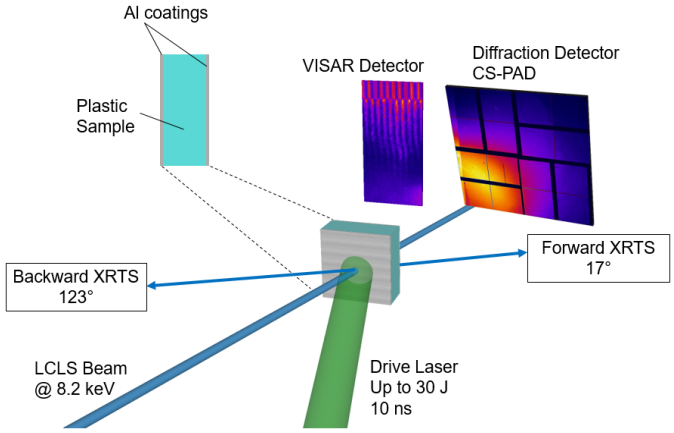

FIG. 1: Schematic of the experimental setup at the MEC endstation of LCLS. The high energy laser beam irradiates a plastic sample - either CH (83 μm polystyrene) or CH_2 (77 μm polyethylene) - driving a shock into the target. The conditions reached were monitored by a VISAR setup, and the compressed sample was probed by a single X-ray pulse at 8.2 keV. The scattered X-ray signal was observed by the large area CS-PAD detector.

In this letter, we show single-shot diffraction data from shock-compressed hydrocarbon samples, taken in a beamtime at LCLS. The results are compared to predictions from density functional theory molecular dynamics (DFT-MD) simulations, where they are in excellent agreement at two different pressure conditions within the HED regime.

Our experiment was performed at the Matter in Extreme Conditions endstation of the Linac Coherent Light Source at Stanford National Accelerator Laboratory. The experimental setup used is shown schematically in Figure 1. Samples of CH (83 μm polystyrene) and CH_2 (76 μm polyethylene) were irradiated by either one or both of the long pulse (10 ns) lasers, for intensities of $\sim 2\times10^{12}$ to 1×10^{13} W/cm^2 with shot-to-shot variation of $\sim$10%.

The temperature and pressure conditions expected in the experiment were simulated hydrodynamically using the code package MULTI with the SESAME 7592 equation of state table for CH and 7171 for CH_2, and the measured laser profiles, giving pressures of $\sim$60 and $\sim$190 GPa, with temperatures estimated from equation of state measurements [26]. The pressure estimates on each shot were then revised using a combination of the X-ray diffraction data and a Velocity Interferometer System for Any Reflector (VISAR) system on the rear side. Further experimental details are given in the Supplementary Material, and in our previous publication [14].

The sample was probed by the XFEL beam close to the breakout time of the shock, such that the conditions were as uniform as possible and maximising the volume of shocked material. In all cases, the shock breakout time was shorter than the laser pulse length, such that the shock was supported throughout. The diffracted signal was observed on a Cornell-SLAC Pixel Array Detector (CS-PAD), covering an angular range of 20°- 90°. This detector is not able to distinguish elastic and inelastic scattering at a given angle, where the latter can be due to collective effects (i.e. plasmon scattering) at small angles, or Compton scattering at larger angles. To account for this, the MCSS (Multicomponent Scattering Simulation) code [27, 28] was used to calculate the inelastic signal as a function of the scattering angle, which was added to the calculated elastic signal described below. To check the validity of this, the predicted spectra were compared to results from X-ray Thomson Scattering (XRTS) spectrometers, deployed at fixed angles (17°and 123°), where the total signal showed good agreement. The value of the elastic scattering as a function of angle arises from the structure of the ions within the sample and means that diffraction measurements can directly compare experimental and simulated results.

For this work, DFT-MD simulations were performed using the VASP package [29], with the temperature and pressure conditions estimated above used as inputs; the specific details of these simulations are given in the Supplementary Material. These runs yield the positions of the atoms at each timestep, which can then be Fourier transformed to give the static structure factor $S_{ab}(k)$, describing the spatial correlation between the species (a, b) in equilibrium, including both the self-correlation S_{CC}, S_{HH} and inter-species correlation S_{CH}.

Relating this to the experimental parameters, the wavevector $k = (4\pi/\lambda)\sin(\theta/2)$, where λ is the wavelength of the probing X-rays and θ the scattering angle. The value measured in the experiment is the Rayleigh weight, which is proportional to the X-ray intensity elastically scattered from the sample at a given wavevector [11]

$$W_R(k) = \sum_{a,b} \sqrt{x_a x_b}\, f_a(k) f_b(k)\, S_{ab}(k). \qquad (1)$$

The form factor $f_i(k)$ describes the distribution of bound electrons around the ions and is extracted from the DFT-MD simulations; this expression ignores the effect of the screening factor $q_i(k)$, describing free electron contributions, as it is negligible at the conditions considered [21]. The value x_a is the number ratio of the species $x_a = N_a/\sum_i N_i$.

Figure 2 shows the a) structure factors and b) Rayleigh weights for a pure carbon sample (solid line), and for the different correlation components of a CH sample (dashed lines). The two-peak structure is characteristic of liquid

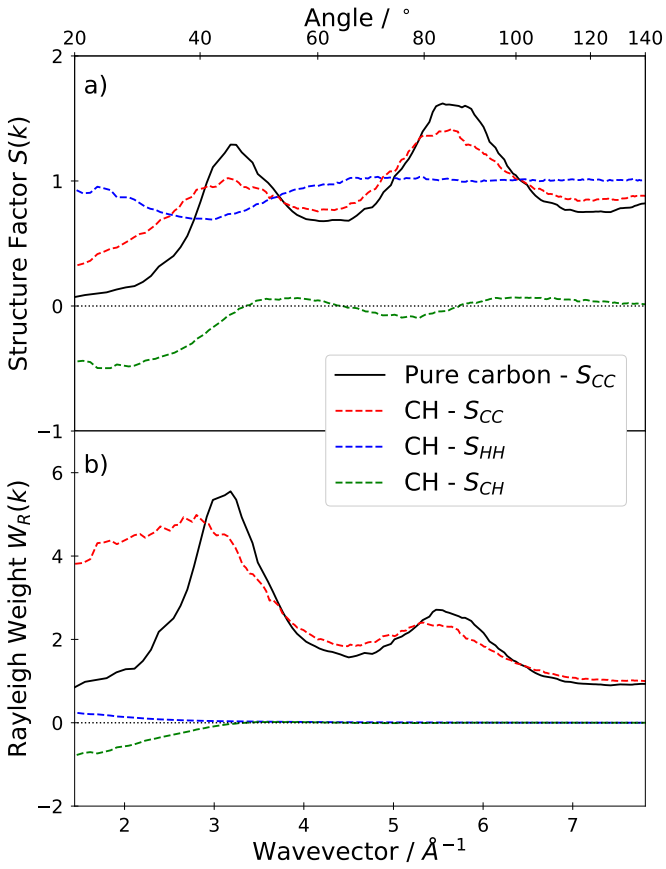

FIG. 2: Simulated values for the a) structure factor and b) Rayleigh weight from mixed CH and pure carbon simulations at 150 GPa and 6000 K. In both cases, the carbon-carbon component exhibits the characteristic two-peak structure, with the screening effect of the hydrogen in the mixed case leading to less strong correlations. The carbon-carbon correlations dominate the Rayleigh weight due to the form factor $f(k)$, which is proportional to the number of electrons around the ion.

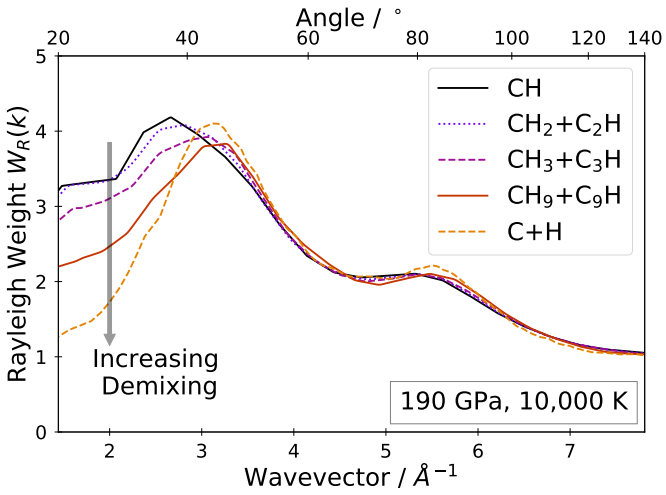

FIG. 3: Simulated values for the Rayleigh weight from a CH sample with increasing degrees of demixing, at 190 GPa and 10,000 K. For moderate degrees of demixing, the change in the total signal is too small to be confidently distinguished from the completely mixed case.

carbon [30], and is due to residual bonding that persists after melting. In the case of CH, a similar shape can be seen in the carbon-carbon structure factor, which dominates the overall signal of the Rayleigh weight due to the much larger value for the form factor of carbon, relative to hydrogen.

Similar simulations can be performed for samples with different carbon-hydrogen ratios, and combined to demonstrate the effect of demixing on the expected diffraction signal. Instead of taking the result of e.g., a single mixed simulation of carbon and hydrogen in a 1:1 ratio, outputs from two simulations with different ratios, which sum to the original ratio, can be combined. These results are shown in Figure 3, for CH and increasingly asymmetrically demixed regions. We see that, as the material demixes, the first peak sharpens and the signal at low k decreases, approaching that of a pure carbon liquid sample. However, this change only becomes significant when the ratio in the carbon region is above at least 3:1, and so moderate levels of demixing cannot be distinguished by diffraction in this material. A similar ambiguity is found for the case of CH_2. We should stress that in none of the simulations performed was spontaneous demixing observed, and that therefore all of the 'demixed' theoretical results are in fact a combination of mixed results at different ratios. That demixing does not seem to spontaneously occur within the simulation box, however, may be due to the limited number of particles considered, and the possible runtime compared to the demixing timescale.

The experimental results are shown as solid lines in Figure 4, with the shaded region showing the range of shots at the same nominal laser drive conditions. To directly compare the simulated and experimental data, the DFT-MD data (Rayleigh peak) also includes the modeled effect of the angle-dependent inelastic scattering. The experimental data is scaled to remove the effect of absorption within the target and the detector shielding, and the effect of the polarization of the probing XFEL beam was accounted for in the Dioptas software [31] used to analyse the CS-PAD data.

Looking first at the pre-shock (cold) data from each sample (dotted lines in Figure 4), it is clear that the CH has no Bragg peaks, and is dominated by a steep rise in signal at low angles, whereas the CH_2 has a complex

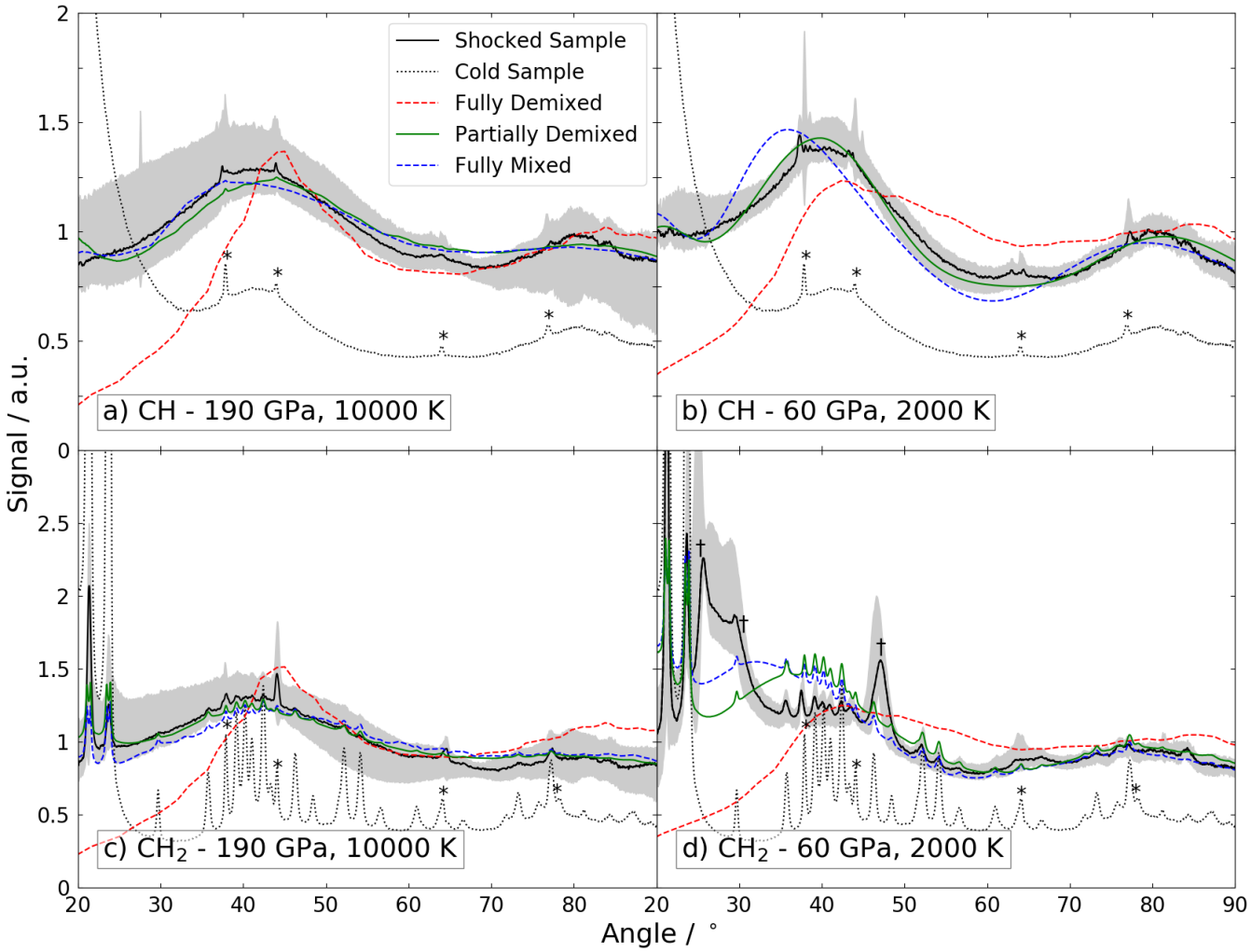

FIG. 4: Azimuthally integrated lineouts of the diffraction data from the CS-PAD, compared to DFT-MD simulations with mixed and demixed hydrocarbons. The black lines show single shots, and the shaded regions around them indicate the range of data at similar shock conditions, normalized to the on-shot X-ray intensity. The partially demixed result is the best-fitting case of the combinations shown in Figure 3 at the appropriate conditions. The dotted line indicates the initial structure of the sample, before laser irradiation, with peaks from Al marked by *. In the case of the lower pressure CH_2 data, locations of Bragg peaks attributed to the monoclinic *A2/m* structure at a pressure of 47 GPa are indicated by †.

crystal structure, primarily orthorhombic *Pnam* [32]. In both cases, Bragg diffraction lines from the thin (100 nm) Al layers on either side of the target are also seen, marked by * in Figure 4, although these disappear completely in shots probing after the shock has broken out the rear side of the sample.

After compression (solid black lines), the structures are more similar, with all except Figure 4d) showing a liquid structure with two broad peaks in the angular range probed. The exception to this is the case of weakly shocked CH_2 where at least three new peaks (relative to the cold diffraction data) are present in the lineout and are marked by †. These appear to be due to a monoclinic *A2/m* crystal structure, which was previously found to be the most stable structure above 14 GPa [32]. The lattice parameters are taken from Fontana *et al.* and scaled hydrostatically, using the compressibility estimates from the paper, such that the position of the strong peak at 47° in Figure 4d) is fitted. We expect that better agreement with the lower two peaks could be found by varying the lattice parameters independently, but this is beyond the scope of this work.

CH_2 at both pressures measured also contains obvious signal from the initial crystal structure, with the Bragg peaks at 21°and 23° still particularly visible. This is due to a 'halo' of X-rays around the focal spot, comprising

∼5% of the total fluence, which gives diffraction signal from cold material outside the shocked region even at long delays. This cold signal also appeared in the CH shots, but has been subtracted to better demonstrate the fitting with the theoretical lineouts.

The liquid structures predicted by the DFT-MD simulations are very similar to those present in the data for all the target/pressure combinations where liquid structure dominates. The shapes, positions and heights of the liquid peaks agree very closely with the results, although this is true for both fully and partially mixed simulations. The fully demixed case, calculated assuming separate regions of pure carbon and hydrogen, diverges significantly from the data at low k, and therefore such extreme demixing behaviour can be ruled out. In the weakly shocked CH_2, the data agrees at higher angles, where smaller scale effects dominate, but at lower angles there is a clear redistribution of signal from the broad liquid peak into specific lattice peaks, which were not present in the DFT-MD simulations.

Although previous work had suggested that diffraction would be an appropriate technique to observe demixing in liquid-like warm dense matter [11], our results demonstrate that this is not necessarily the case. For the samples and conditions probed, the overall structure factor changes very little with moderate demixing, i.e. regions with an atomic imbalance of up to around 3:1. For CH at the strong shock conditions, the simulated Rayleigh weight – defined in Equation (1) – is plotted for different degrees of demixing in Figure 3. At ratios in the carbon-enriched region of up to 3:1, the maximum change in signal is on the order of 10%. Although our data can rule out regions with carbon ratios above C_9H at the conditions reached, weaker demixing effects are still sufficient to give density variations that could, for instance, seed observed instabilities and fuel-ablator mixing in inertial confinement fusion capsule implosions [6, 10, 15]. While diffraction cannot distinguish the small differences in structure between these regions, diagnostics sensitive to density gradients, such as SAXS [33], may be useful for better constraining this in the future.

To conclude, it is clear that X-ray diffraction is an important method for observing the structure of high energy density samples, and our results demonstrate that single-shot data can be obtained even in low-Z materials without strong structural order. At pressure-temperature conditions reached by a single shock in CH targets, the liquid structure agrees very well with that predicted from DFT-MD simulations. In CH_2, crystalline structures persist at pressures around 60 GPa on the timescales probed in this experiment, but do not remain at 190 GPa. These results are good validation for the prediction of liquid structure in HED mixtures, and are promising for future work looking at novel structures in other low-Z elements and compounds at planetary interior conditions. While the lack of complete demixing is promising for ICF implosions, we cannot rule out other chemical activity and partial demixing, and it may therefore be useful for future studies to use additional diagnostics which can better resolve density inhomogeneities.

This work was performed at the Matter at Extreme Conditions (MEC) endstation of the Linac Coherent Light Source (LCLS), SLAC National Accelerator Laboratory, supported by the U.S. Department of Energy (DOE), Office of Science, Office of Basic Energy Sciences under Contract No. DE-AC02-76SF00515. The MEC instrument has additional support from the DOE, Office of Science, Office of Fusion Energy Sciences under contract No. SF00515. N.J.H., K.R., A.K.S. and D.K. were supported by the Helmholtz Association under VH-NG-1141. N.J.H. was supported in part by JSPS KAKENHI Grant No. 16K17846. The work of T.D., A.P. and S.F. was performed under the auspices of the U.S. Department of Energy by Lawrence Livermore National Laboratory under Contract DE-AC52-07NA27344. T.D. was supported by Laboratory Directed Research and Development (LDRD) Grant No. 18-ERD-033. S.F. was supported by Bundesministerium für Bildung und Forschung (BMBF) with project no. 05P15RDFA1. The MCSS code is (C) British Crown Owned Copyright 2017/AWE and is used with permission.

* n.hartley@hzdr.de

[1] N. Nettelmann,Predictions on the core mass of Jupiter and of giant planets in general, Astrophysics and Space Science 336 (1) (2011) 47–51.

[2] F. Soubiran, B. Militzer, K. P. Driver, S. Zhang, Properties of hydrogen , helium , and silicon dioxide mixtures in giant planet interiors, Physics of Plasmas 24 (4) (2017) 041401.

[3] M. Millot, S. Hamel, J. R. Rygg, P. M. Celliers, G. W. Collins, F. Coppari, D. E. Fratanduono, R. Jeanloz, D. C. Swift, J. H. Eggert, Experimental evidence for superionic water ice using shock compression, Nature Physics 14 (2018) 297-302.

[4] H. K. Mao, Y. Wu, L. C. Chen, J. F. Shu, A. P. Jephcoat, Static Compression of Iron to 300 GPa and FeNi Alloy to 260 GPa: Implications for Composition of the Core, Journal of Geophysical Research 95 (B13) (1990) 737–742.

[5] D. K. Spaulding, R. S. McWilliams, R. Jeanloz, J. H. Eggert, P. M. Celliers, D. G. Hicks, G. W. Collins, R. F. Smith, Evidence for a Phase Transition in Silicate Melt at Extreme Pressure and Temperature Conditions, Physical Review Letters 108 (6) (2012) 065701.

[6] R. S. Craxton, K. S. Anderson, T. R. Boehly, V. N. Goncharov, D. R. Harding, J. P. Knauer, R. L. McCrory, P. W. McKenty, D. D. Meyerhofer, J. F. Myatt, A. J. Schmitt, J. D. Sethian, R. W. Short, S. Skupsky, W. Theobald, W. L. Kruer, K. Tanaka, R. Betti, T. J. B. Collins, J. A. Delettrez, S. X. Hu, J. A. Marozas, A. V. Maximov, D. T. Michel, P. B. Radha, S. P. Regan, T. C. Sangster, W. Seka, A. A. Solodov, J. M. Soures, C. Stoeckl, J. D. Zuegel, Direct-drive inertial confinement

fusion: A review, Physics of Plasmas 22 (11) (2015).
[7] A. L. Kritcher, T. Döppner, D. Swift, J. A. Hawreliak, G. Collins, J. Nilsen, B. L. Bachmann, E. Dewald, D. Strozzi, S. Felker, O. L. Landen, O. Jones, C. Thomas, J. Hammer, C. Keane, H. Lee, S. H. Glenzer, S. Rothman, D. A. Chapman, D. Kraus, P. Neumayer, R. W. Falcone, Probing matter at Gbar pressures at the NIF, High Energy Density Physics 10 (2014) 27–34.
[8] W. B. Hubbard, W. J. Nellis, A. C. Mitchell, N. C. Holmes, P. C. McCandless, S. S. Limaye,Interior structure of Neptune - Comparison with Uranus, Science 253 (5020) (1991) 648.
[9] I. Prencipe, J. Fuchs, S. Pascarelli, D. Schumacher, R. Stephens, N. B. Alexander, R. Briggs, M. Büscher, M. Cernaianu, A. Choukourov, M. De Marco, A. Erbe, J. Fassbender, G. Fiquet, P. Fitzsimmons, C. Gheorghiu, J. Hund, L. Huang, M. Harmand, N. J. Hartley, A. Irman, T. Kluge, Z. Konopkova, S. Kraft, D. Kraus, V. Leca, D. Margarone, J. Metzkes, K. Nagai, W. Nazarov, P. Lutoslawski, D. Papp, M. Passoni, A. Pelka, J. Perin, J. Schulz, M. Smid, C. Spindloe, S. Steinke, R. Torchio, C. Vass, T. Wiste, R. Zaffino, K. Zeil, T. Tschentscher, U. Schramm, T. Cowan, Targets for high repetition rate laser facilities: Needs, challenges and perspectives, High Power Laser Science and Engineering 5 (e17) (2017).
[10] A. Kritcher, D. Clark, S. Haan, S. Yi, A. Kritcher, S. Haan, S. Yi, A. Zylstra, J. Ralph, C. Weber, Comparison of the Three NIF Ablators, Tech. rep. (2017).
[11] K. Wünsch, J. Vorberger, G. Gregori, D. O. Gericke, X-ray scattering as a probe for warm dense mixtures and high-pressure miscibility, EPL 94 (2011) 25001.
[12] M. A. Morales, S. Hamel, K. J. Caspersen, E. Schwegler, Hydrogen-helium demixing from first principles: From diamond anvil cells to planetary interiors, Physical Review B 87 (17) (2013) 5–8.
[13] N. Nettelmann, B. Holst, A. Kietzmann, M. French, R. Redmer, D. Blaschke, Ab Initio Equation of State Data for Hydrogen, Helium, and Water and the Internal Structure of Jupiter, The Astrophysical Journal 683 (2) (2008) 1217–1228.
[14] D. Kraus, J. Vorberger, A. Pak, N. J. Hartley, L. B. Fletcher, S. Frydrych, E. Galtier, E. J. Gamboa, D. O. Gericke, S. H. Glenzer, E. Granados, M. J. MacDonald, A. J. MacKinnon, E. E. McBride, I. Nam, P. Neumayer, M. Roth, A. M. Saunders, A. K. Schuster, P. Sun, T. van Driel, T. Döppner, R. W. Falcone, Formation of diamonds in laser-compressed hydrocarbons at planetary interior conditions, Nature Astronomy 1 (September) (2017).
[15] C. D. Orth, Spallation as a dominant source of pusher-fuel and hot-spot mix in inertial confinement fusion capsules, Physics of Plasmas 23 (2) (2016) 022706.
[16] N. Nettelmann, K. Wang, J. J. Fortney, S. Hamel, S. Yellamilli, M. Bethkenhagen, R. Redmer,Uranus evolution models with simple thermal boundary layers , Icarus 275 (2016) 107–116.
[17] L. Dubrovinsky, N. Dubrovinskaia, V. B. Prakapenka, A. M. Abakumov,Implementation of micro-ball nanodiamond anvils for high-pressure studies above 6 Mbar, Nature Communications 3 (2012) 1163–1167.
[18] S. Petitgirard, A. Salamat, P. Beck, G. Weck, P. Bouvier, Strategies for in situ laser heating in the diamond anvil cell at an X-ray diffraction beamline, Journal of Synchrotron Radiation 21 (1) (2014) 89–96.
[19] M. D. Knudson, M. P. Desjarlais, Shock compression of quartz to 1.6 TPa: Redefining a pressure standard, Physical Review Letters 103 (22) (2009) 5–8.
[20] M. Koenig, E. Henry, G. Huser, A. Benuzzi-Mounaix, B. Faral, E. Martinolli, S. Lepape, T. Vinci, D. Batani, M. Tomasini, B. Telaro, P. Loubeyre, T. Hall, P. Celliers, G. Collins, L. DaSilva, R. Cauble, D. Hicks, D. Bradley, A. MacKinnon, P. Patel, J. Eggert, J. Pasley, O. Willi, D. Neely, M. Notley, C. Danson, M. Borghesi, L. Romagnani, T. Boehly, K. Lee, High pressures generated by laser driven shocks: applications to planetary physics, Nuclear Fusion 44 (12) (2004) S208–S214.
[21] S. H. Glenzer, R. Redmer,X-ray Thomson scattering in high energy density plasmas, Reviews of Modern Physics 81 (4) (2009) 1625–1663.
[22] L. Fletcher, H. Lee, T. Döppner, E. Galtier, B. Nagler, P. A. Heimann, C. Fortmann, S. LePape, T. Ma, M. Millot, A. Pak, D. Turnbull, D. A. Chapman, D. Gericke, J. Vorberger, T. G. White, G. Gregori, M. Wei, B. Barbrel, R. W. Falcone, C. Kao, H. Nuhn, J. Welch, U. Zastrau, P. Neumayer, J. B. Hastings, S. H. Glenzer, Ultrabright X-ray laser scattering for dynamic warm dense matter physics, Nature Photonics 9 (4) (2015) 274–279.
[23] O. T. Lord, I. G. Wood, D. P. Dobson, L. Vočadlo, W. Wang, A. R. Thomson, E. T. H. Wann, G. Morard, M. Mezouar, M. J. Walter, The melting curve of Ni to 1 Mbar, Earth and Planetary Science Letters 408 (2015) 226–236.
[24] D. Kraus, A. Ravasio, M. Gauthier, D. O. Gericke, J. Vorberger, S. Frydrych, J. Helfrich, L. Fletcher, G. Schaumann, B. Nagler, B. Barbrel, B. Bachmann, E. J. Gamboa, S. Göde, E. Granados, G. Gregori, H. Lee, P. Neumayer, W. Schumaker, T. Döppner, R. W. Falcone, S. H. Glenzer, M. Roth,Nanosecond formation of diamond and lonsdaleite by shock compression of graphite, Nature Communications 7 (2016) 10970.
[25] G. Weck, F. Datchi, G. Garbarino, S. Ninet, J. A. Queyroux, T. Plisson, M. Mezouar, P. Loubeyre, Melting curve and liquid structure of nitrogen probed by x-ray diffraction to 120 GPa, Physical Review Letters 119 (23) (2017) 235701.
[26] M. A. Barrios Garcia,Precision equation of state measurements on hydrocarbons in the high energy density regime, Ph.D. thesis, University of Rochester (2010).
[27] D. A. Chapman, Probing the dynamic response of dense matter with x-ray Thomson scattering, Ph.D. thesis, University of Warwick (2015).
[28] D. A. Chapman, User Guide and Theoretical Basis for the Multi-Component Scattering Spectra (MCSS) Thomson Scattering Analysis Code, Tech. rep., AWE Report 12/17, AWE (2017).
[29] J. Hafner, Ab initio simulations of materials using VASP: Density functional theory and beyond., Journal of Computational Chemistry 29 (13) (2008).
[30] D. Kraus, J. Vorberger, D. Gericke, V. Bagnoud, A. Blažević, W. Cayzac, A. Frank, G. Gregori, A. Ortner, A. Otten, F. Roth, G. Schaumann, D. Schumacher, K. Siegenthaler, F. Wagner, K. Wünsch, M. Roth,Probing the Complex Ion Structure in Liquid Carbon at 100 GPa, Physical Review Letters 111 (25) (2013) 255501.
[31] C. Prescher, V. B. Prakapenka, DIOPTAS: a program for reduction of two-dimensional X-ray diffraction data and

data exploration, High Pressure Research 35 (3) (2015) 223–230.

[32] L. Fontana, D. Q. Vinh, M. Santoro, S. Scandolo, F. A. Gorelli, R. Bini, M. Hanfland, High-pressure crystalline polyethylene studied by x-ray diffraction and ab initio simulations, Physical Review B 75 (2007) 174112.

[33] T. Kluge, C. Rödel, M. Rödel, A. Pelka, E. E. McBride, L. B. Fletcher, M. Harmand, A. Krygier, A. Higginbotham, M. Bussmann, E. Galtier, E. Gamboa, A. L. Garcia, M. Garten, S. H. Glenzer, E. Granados, C. Gutt, H. J. Lee, B. Nagler, W. Schumaker, F. Tavella, M. Zacharias, U. Schramm, T. E. Cowan, Nanometer-scale characterization of laser-driven compression, shocks, and phase transitions, by x-ray scattering using free electron lasers, Physics of Plasmas 24 (10) (2017) 102709.